The Astrophysical Journal, 748:97 (13pp), 2012 April 1 doi:10.1088/0004-637X/748/2/97

WHAT SETS THE INITIAL ROTATION RATES OF MASSIVE STARS?

Anna L. Rosen, Mark R. Krumholz, and Enrico Ramirez-Ruiz
Department of Astronomy and Astrophysics, University of California Santa Cruz, 211 Interdisciplinary Sciences Building, 1156 High Street, Santa Cruz, CA 95064, USA; rosen@ucolick.org

Received 2011 November 18; accepted 2012 January 16; published 2012 March 13

ABSTRACT

The physical mechanisms that set the initial rotation rates in massive stars are a crucial unknown in current star formation theory. Observations of young, massive stars provide evidence that they form in a similar fashion to their low-mass counterparts. The magnetic coupling between a star and its accretion disk may be sufficient to spin down low-mass pre-main-sequence (PMS) stars to well below breakup at the end stage of their formation when the accretion rate is low. However, we show that these magnetic torques are insufficient to spin down massive PMS stars due to their short formation times and high accretion rates. We develop a model for the angular momentum evolution of stars over a wide range in mass, considering both magnetic and gravitational torques. We find that magnetic torques are unable to spin down either low-mass or high-mass stars during the main accretion phase, and that massive stars cannot be spun down significantly by magnetic torques during the end stage of their formation either. Spin-down occurs only if massive stars' disk lifetimes are substantially longer or their magnetic fields are much stronger than current observations suggest.

Key words: stars: formation – stars: magnetic field – stars: massive – stars: protostars – stars: rotation

Online-only material: color figures

1. INTRODUCTION

While there has been significant theoretical attention to understanding the initial rotation rates of Sun-like stars, far less work has been done on more massive stars. Since the stellar evolutionary path depends on the rate of mass loss and internal mixing, both of which are enhanced by rotation (Bjorkman & Cassinelli 1993; Maeder & Meynet 2010), our inability to predict initial rotation rates is a limiting factor in stellar evolution theory. Observations of young, massive stars provide evidence that they form in a similar fashion to their low-mass counterparts: via gravitational collapse of a molecular cloud core (McKee & Tan 2003; Zapata et al. 2008; Davies et al. 2011). These cloud cores are slowly rotating but have very large radii, and thus have high initial angular momenta. This has led to the "angular momentum problem" in which the initial angular momentum of a cloud core is at least three orders of magnitude greater than the resulting star (Goodman et al. 1993; Bodenheimer 1995; Larson 2010) and must be redistributed or removed during collapse.

Massive stars form in magnetized high-density turbulent gas clumps (Crutcher 1999) that are characterized by short core-collapse times and high time-averaged accretion rates (McKee & Tan 2003). Due to the high angular momentum content of the diffuse gas, material is unable to be directly deposited on to the central object and is instead circularized at a distance far from the star, resulting in a disk (Krumholz et al. 2007, 2009). Observations, although rare, confirm that disks form around massive protostars during cloud collapse (Cesaroni et al. 2006, 2007; Chini et al. 2011) and the accretion onto these disks is regulated at least in part by the magnetic field (Vlemmings et al. 2010). Furthermore, these disks might evolve like those located around young, low-mass stars (Chini et al. 2006). The disk transfers mass and angular momentum to the central protostar, which acts to spin it up. This transfer of angular momentum, along with contraction of the protostar toward the main sequence, suggests that young stars should be rotating at or near their breakup speed, the rotational speed at which the centripetal force at the equator balances gravity.

Lin et al. (2011) found that gravitational torques prohibit a star from rotating above ∼50% of its breakup speed during formation. However, the observed projected rotation rates of young low-mass and some massive stars suggest that they rotate at a much lower fraction. Observations of low-mass pre-main-sequence (PMS) stars suggest that their rotation periods span a factor of ∼30 and approximately half are slow rotators, rotating at about 10% of their breakup speed (Hartmann & Stauffer 1989; Herbst et al. 2007). The observed rotational velocities of massive stars suggest that they are spinning significantly faster than their low-mass counterparts. Wolff et al. (2006) studied a sample of young massive stars ($M_\star > 25\ M_\odot$) and found that their median rotation rate was 20% of their breakup speed. Huang et al. (2010) observed the projected rotational velocity distribution of 220 young B stars and found that approximately 53.3% are rapid rotators, rotating with a velocity that is at least 40% of their breakup speed. How these initial rotation rates are achieved and their dependence on stellar mass are still unanswered questions.

The physical mechanism responsible for causing young low-mass stars to be slow rotators has received considerable attention over the last three decades. One popular theory is that during the T Tauri phase (experienced by PMS stars with masses less than $\sim 3\ M_\odot$), when the accretion rate is low, $\dot{M}_a \lesssim 10^{-7}\ M_\odot\ \mathrm{yr}^{-1}$ (Hartmann et al. 2006), the magnetic connection between the star and its accretion disk can transport substantial angular momentum away from the star, resulting in spin rates well below breakup in agreement with observations (Koenigl 1991; Armitage & Clarke 1996). The fact that T Tauri stars have strong magnetic fields, typically several hundred G to several kG (Johns-Krull 2007), long contraction timescales after their main assembly, and long accretion disk lifetimes supports this spin-down scenario (Bouvier 2007). However, Matt & Pudritz (2005) and Matt et al. (2010) found that when the stellar magnetic field lines open due to the differential twisting between the star and

disk the resulting rotation rates, while still below breakup, are higher than those of the slowest rotators.

Magnetic fields have been detected in a small sample of young and evolved OB stars. These fields are between a few hundred G to several kG and typically have a bipolar topology (Donati et al. 2006; Wade et al. 2006; Hubrig et al. 2008; Grunhut et al. 2009; Martins et al. 2010). The origin of these fields is poorly understood, since the envelopes of such stars are radiative rather than convective, excluding the possibility of a solar-type dynamo effect (Moss 2001). The favored hypothesis for the presence of magnetic fields in massive stars is that they are fossil fields that were either accumulated or generated during star formation (Walder et al. 2011). Alecian et al. (2008) discovered two very young B stars with strong surface magnetic fields. They found that the younger of the two is a rapid rotator and situated in the first half of the PMS phase, whereas the older star, which might already be on the main sequence, is a slow rotator most likely spun down via magnetic torques.

This implies that massive stars likely have strong magnetic fields present during their formation and that these fields, due to coupling with the accretion disk, may be able to remove a substantial amount of angular momentum from the star, producing spin rates on the zero-age main sequence (ZAMS) well below breakup in a similar fashion to their low-mass counterparts. However, massive stars reach the ZAMS very quickly since they have short thermal equilibrium timescales. They also have higher accretion rates during their formation and their magnetic fields are weaker relative to their stellar binding energy as compared to low-mass stars. They likely have shorter disk lifetimes than contracting low-mass stars, since their disks are likely to be quickly photodisintegrated due to their high luminosities (Cesaroni et al. 2007). All of these factors make magnetic spin-down more difficult. In this paper, we explore whether the initial spins of massive stars are regulated by the interaction of their accretion disk with the stellar magnetic field. To study this issue, we model the angular momentum evolution for both low-mass and massive protostars by considering both magnetic and gravitational torques. We apply the star–disk interaction model developed by Matt & Pudritz (2005, hereafter MP05), where the stellar magnetic field is connected to a finite region of the accretion disk, and the twisting of the magnetic field lines due to the differential rotation between the star and disk leads to a spin-down torque on the star.

This paper is organized as follows. In the following section (Section 2), we give a brief introduction to how the presence of surface magnetic fields during the protostellar phase can extract angular momentum from the star. We describe our stellar angular momentum evolution model, which includes a prescription for protostellar evolution and the star–disk interaction, in Section 3. We state our results in Section 4. Lastly, we discuss our results in Section 5.

2. MAGNETIC TORQUES: THEORY AND BACKGROUND

Protostars embedded in circumstellar disks accrete material from an angular momentum–rich mass reservoir. If the disk is Keplerian, the specific angular momentum content of the circulating material, $j = \sqrt{GM_\star r}$, increases outward and the angular velocity increases inward. The presence of a stellar magnetic field is able to disrupt the disk outside the stellar radius and channel the disk material along field lines. Spin-down torques will be conveyed to the star due to the differential twisting of the field lines threading the accretion disk at radii where the disk rotates at a lower rate than the star. In this section, we give simple scaling arguments to demonstrate how spin evolution varies with stellar mass, before proceeding to a more detailed numerical model in Section 3. The derivation that follows is an oversimplification and ensures maximum spin-down via magnetic braking. We include this section for the reader who is unfamiliar with the literature.

The radial extent of the accretion disk can be altered if the protostar has a magnetic field. The magnetic field is able to truncate the disk at the Alfvén radius (denoted $R_{\rm A}$) where the magnetic pressure, $B^2/8\pi$, balances the ram pressure, ρv^2, of the infalling material. Assuming that the stellar magnetic field is dipolar and the magnetic field axis is aligned with the rotation axis of the star, the z component of the field in the equatorial plane at a distance r from the star is given by

$$B_{\rm z} = B_\star \left(\frac{r}{R_\star}\right)^{-3}, \tag{1}$$

where $B_\star$ is the magnetic field strength at the stellar surface. The location at which the magnetic pressure is able to truncate the disk, assuming spherical free-fall accretion, is

$$\frac{R_{\rm A}}{R_\star} = 2.26 \left(\frac{B_\star}{2\,{\rm kG}}\right)^{4/7} \left(\frac{\dot{M}_{\rm a}}{10^{-7}\,M_\odot\,{\rm yr}^{-1}}\right)^{-2/7} \times \left(\frac{M_\star}{M_\odot}\right)^{-1/7} \left(\frac{R_\star}{R_\odot}\right)^{5/7}, \tag{2}$$

where $\dot{M}_{\rm a}$ is the accretion rate. In the case of disk accretion, the truncation radius is in general smaller than the value given in Equation (2) by a factor of order unity. For simplicity and for the purpose of this section we neglect this factor in the following discussion.

If the stellar magnetic field lines are connected to the disk, the differential rotation between the two will cause the field lines to twist in the azimuthal direction, inducing torques on the star. The disk corotates with the star at the location $R_{\rm co} \equiv (GM_\star)^{1/3}\,\Omega_\star^{-2/3}$, where $\Omega_\star$ is the angular velocity of the star. The stellar field lines that connect to the disk outside the $R_{\rm co}$ spin up the disk and spin down the star. If the field lines connect to a significant portion of the disk outside of $R_{\rm co}$, the star can be spun down to a velocity well below its breakup speed.

The stellar magnetic field lines threading an annulus of the accretion disk with width dr will exert a torque:

$$d\tau_{\rm m} = B_\phi B_{\rm z} r^2 dr, \tag{3}$$

where B_ϕ is the azimuthal component of the field generated by the twisting of the field lines relative to the star and is given by

$$B_\phi = B_z \frac{\Omega(r) - \Omega_\star}{\Omega(r)}, \tag{4}$$

where Ω is the angular velocity of the Keplerian accretion disk. Integrating Equation (3) from $R_{\rm A}$ to infinity, the total torque on the star due to the stellar magnetic field lines connected to the disk is

$$\tau_{\rm m} = \frac{B_\star^2 R_\star^6}{3}\left(R_{\rm A}^{-3} - 2R_{\rm co}^{-3/2} R_{\rm A}^{-3/2}\right). \tag{5}$$

The accretion of disk material at $R_{\rm A}$ adds angular momentum to the star at a rate

$$\tau_{\rm a} = \dot{M}_{\rm a}\sqrt{GM_\star R_{\rm A}}. \tag{6}$$

Note that Equation (5) contains both spin-up and spin-down torques acting on the star due to field lines connected to the disk within and outside of $R_{\rm co}$, respectively. In order for the net magnetic torque to transport angular momentum away from the star (i.e., $\tau_{\rm m} < 0$), $R_{\rm A}$ must be greater than

$$R_{\rm A,\,min} \approx 0.63 R_{\rm co}. \quad (7)$$

In a system where the stellar parameters ($M_\star$, $R_\star$, $B_\star$, $\dot{M}_{\rm a}$) are relatively constant there exists an equilibrium state, called the "disk-locked" state (Koenigl 1991; Armitage & Clarke 1996; Matt & Pudritz 2005), in which the stellar spin rate will adjust to its equilibrium value (i.e., when $\tau_a + \tau_m = 0$). Setting $\tau_{\rm a} = -\tau_{\rm m}$, the equilibrium spin rate, as a fraction of the breakup speed ($\Omega_{\rm bu} = \sqrt{GM_\star/R_\star^3}$), is

$$\frac{\Omega_{\star,\rm eq}}{\Omega_{\rm bu}} = \frac{1}{2}\left(\frac{R_{\rm A}}{R_\star}\right)^{-3/2}\left[0.014\left(\frac{M_\star}{M_\odot}\right)^{1/2}\left(\frac{\dot{M}_{\rm a}}{10^{-7}\,M_\odot\,{\rm yr}^{-1}}\right)\times\left(\frac{B_\star}{2\,{\rm kG}}\right)^{-2}\left(\frac{R_{\rm A}}{R_\star}\right)^{7/2}+1\right]. \quad (8)$$

Assuming that the moment of inertia of the star stays constant, the characteristic timescale to reach equilibrium is

$$t_{\star,\rm eq} = k^2 M_\star R_\star^2\left(\frac{\Omega_{\star,\rm eq}-\Omega_\star}{\tau_{\rm a}+\tau_{\rm m}}\right), \quad (9)$$

where k is the dimensionless radius of gyration whose value depends on the stellar structure. Equation (7) only holds when $R_{\rm A} > R_\star$, which is true if the star has a surface magnetic field strength above a minimum value:

$$B_\star > 400\left(\frac{\dot{M}_{\rm a}}{10^{-7}\,M_\odot\,{\rm yr}^{-1}}\right)^{1/2}\left(\frac{M_\star}{M_\odot}\right)^{1/4}\left(\frac{R_\star}{R_\odot}\right)^{-5/4} G. \quad (10)$$

Figure 1 shows the equilibrium spin rate as a fraction of the star's breakup speed and the corresponding timescales required for a 1 $M_\odot$ star and a 30 $M_\odot$ star to reach equilibrium starting from rotation at breakup, both as a function of the accretion rate. We adopt surface magnetic field strengths of 2 kG similar to observations (Wade et al. 2006; Johns-Krull 2007; Grunhut et al. 2009) and assume $k = 0.27$ for a radiative star (e.g., $n = 3$ polytrope). We adopt radii of 3 $R_\odot$ for the 1 $M_\odot$ star (the typical radius of a T Tauri star of this mass) and 7.76 $R_\odot$ for the 30 $M_\odot$ star (ZAMS value). We consider only accretion rates where the equilibrium spin rate is below the breakup rate. As the accretion rate increases, the equilibrium spin rate approaches the breakup rate and the equilibrium timescale quickly decreases. We find that magnetic torques produce equilibrium spin rates below breakup only for accretion rates below $\dot{M}_{\rm a} \lesssim 5\times10^{-5}\,M_\odot\,{\rm yr}^{-1}$, regardless of the stellar mass. In this regard, low- and high-mass stars are similar. The typical mass accretion rates during the main accretion phase, where the majority of the stellar mass is accreted, for low- and high-mass star formation are $5\times10^{-6}\,M_\odot\,{\rm yr}^{-1}$ (Shu 1977) and $5\times10^{-4}\,M_\odot\,{\rm yr}^{-1}$ (McKee & Tan 2003), respectively. For our adopted field strength, $R_{\rm A}$ for the 30 $M_\odot$ star is within the stellar surface at this accretion rate. In contrast, the disk is truncated very close to the stellar surface for the 1 $M_\odot$ star, leading to an equilibrium spin rate close to breakup. We conclude that disk truncation does not occur for massive stars and is unimportant for low-mass stars during the main accretion phase. At the lower accretion rates that are likely to occur after the main accretion phase ends, we find that low- and high-mass stars differ in that the latter have much longer equilibration timescales than the former due to their larger inertia. For example, the equilibration timescale for the 30 $M_\odot$ star for very low accretion rates is a significant fraction of its stellar lifetime, $t_{\rm ms} = 5.9$ Myr (Parravano et al. 2003). Furthermore, at high accretion rates this timescale is comparable to the star's formation timescale (McKee & Tan 2003), suggesting that massive stars are unable to reach spin equilibrium. To further explore the consequences of this analysis, we follow the angular momentum evolution of massive protostars to determine the physical conditions that are required to spin them down by magnetic torques.

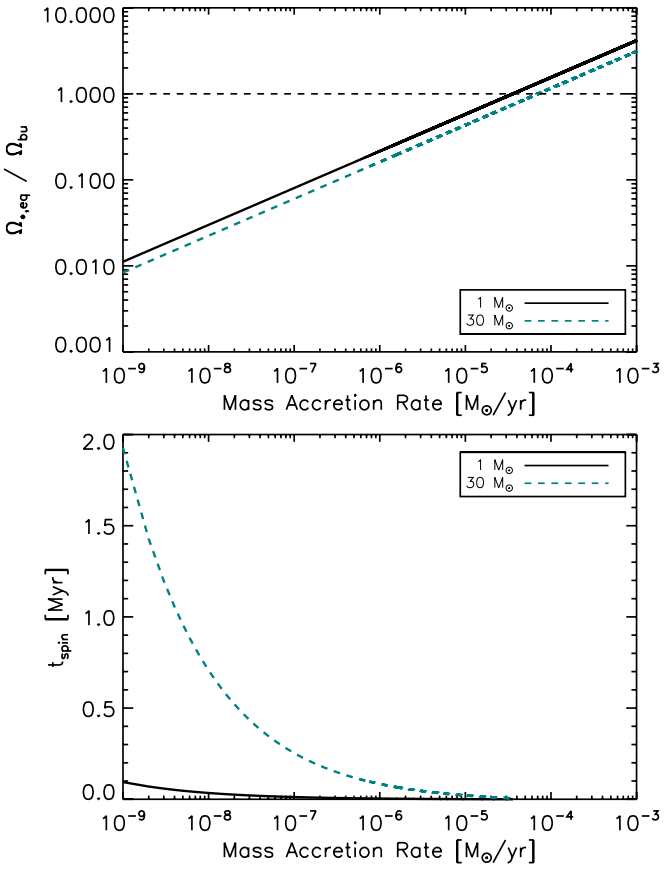

Figure 1. Equilibrium spin rate of a star as a fraction of its breakup spin rate (top panel), and the corresponding spin-down timescale (bottom panel) for 1 $M_\odot$ (black solid line) and 30 $M_\odot$ (teal dashed line) stars to reach equilibrium. Both stars have a surface magnetic field strength of 2 kG with a dipolar topology and are initially rotating at breakup. The horizontal line in the top panel shows where the equilibrium spin rate is equal to the breakup rate.

(A color version of this figure is available in the online journal.)

3. STELLAR ANGULAR MOMENTUM EVOLUTION MODEL

The goal of this work is to determine if the initial rotation rates of massive stars can be regulated by magnetic torques due to the interaction of the stellar magnetic field and surrounding accretion disk during formation. To this end, we construct a simple model to track the mass, radius, and angular momentum content of accreting protostars subjected to gravitational and magnetic torques. We describe the elements of this model in the following subsections.

3.1. Protostellar Model

We monitor the spin and angular momentum evolution by following the protostellar radius and internal structure evolution during its formation with the use of the one-zone model of McKee & Tan (2003, hereafter MT03) as updated by Offner et al. (2009). By treating the protostar as an accreting polytrope and requiring conservation of energy, the evolution of the protostellar radius is given by

$$\frac{dR_\star}{dt} = \frac{2\dot{M}_a R_\star}{M_\star}\left(1 - \frac{1-f_k}{a_g \beta_P} + \frac{1}{2}\frac{d\log\beta_P}{d\log M_\star}\right) - 2\left(\frac{R_\star^2}{GM_\star^2}\right)(L_{int} + L_I - L_D), \quad (11)$$

where $\dot{M}_a$ is the accretion rate onto the protostar, f_k is the fraction of kinetic energy of the infalling material that is radiated away, β_P is the ratio of radiation pressure to the total pressure, $a_g = 3/(5-n)$ is the coefficient describing the binding energy of a polytrope, L_{int} is the internal stellar luminosity, L_I is the rate of energy required to dissociate and ionize the infalling material, and L_D is the rate at which energy is supplied from burning deuterium (Nakano et al. 2000). The model also includes a few discontinuous changes in polytropic index and radius to represent events such as the onset and cessation of core deuterium burning and the formation of a radiative core. We use the model parameters recommended by Offner et al. (2009), which are based on the detailed stellar evolution calculations by Hosokawa & Omukai (2009). We refer the reader to MT03 and Appendix B of Offner et al. (2009) for a detailed description of the model and protostellar evolutionary states.

We treat the protostar as a solid body to follow its angular momentum content ($J_\star = I_\star \Omega_\star$). We evolve the stellar angular momentum content by computing the net torque on the star due to the coupling of the stellar magnetic field with the surrounding accretion disk described in Section 3.3.

3.2. Accretion History

The accretion history of our protostars is divided into two distinct accretion phases. The first is the main accretion phase given by the turbulent core model from MT03, which describes an accelerating accretion rate, where the majority of the stellar mass is accreted. This model assumes that the star-forming core is marginally unstable, massive, and supported by turbulent motions. Next, we follow the disk-clearing phase in which the accretion disk is no longer being fed by the core envelope. These accretion phases are described in Sections 3.2.1 and 3.2.2.

3.2.1. Primary Accretion Phase: Core Collapse

We model the mass accretion using the two-component core model of MT03, which assumes that the central region of a molecular cloud core is dominated by thermal motions and the core envelope is dominated by non-thermal motions (Myers & Fuller 1992). This leads to a density distribution that is equivalent to the sum of a singular polytropic sphere and a singular isothermal sphere:

$$\rho = \rho_s \left(\frac{R_{core}}{r}\right)^{k_\rho} + \frac{c_{th}^2}{2\pi G r^2}, \quad (12)$$

where ρ_s is the density at the surface of the core, R_{core} is the core radius, and c_{th} is the thermal sound speed within the core and is assumed to be constant. We adopt the fiducial value of $k_\rho = 1.5$ from MT03 in agreement with observations describing the turbulence-supported density profile of massive star-forming cores (Caselli & Myers 1995; van der Tak et al. 2000; Beuther et al. 2002).

The accretion rate onto the disk, which is supplied by the background core, is

$$\dot{M}_a \simeq \frac{\phi_\star M_{\star,f}}{t_{\star,ff}}\left[\left(\frac{M_\star}{M_{\star,f}}\right)^{2j} + \left(\frac{\phi_{\star,th}}{\phi_{\star,nth}}\right)^2 \left(\frac{\epsilon_{core} M_{th}}{M_{\star,f}}\right)^{2j}\right], \quad (13)$$

where $t_{\star,ff} = (3\pi/32G\rho)^{1/2}$ is the free-fall time evaluated at R_{core}, $M_\star$ is the current stellar mass, $M_{\star,f}$ is the final stellar mass, and

$$j = \frac{3(2-k_\rho)}{2(3-k_\rho)}. \quad (14)$$

The dimensionless constants ϕ, $\phi_{\star,th}$, and $\phi_{\star,nth}$ are of order unity and depend on k_ρ and the magnetic field strength. The efficiency factor, ϵ_{core}, describes how much of the core mass will end up in the star rather than being ejected by the protostellar outflow, and we adopt the value of 0.5 from MT03, which is typical of both low-mass (Matzner & McKee 2000) and high-mass star formation (Cunningham et al. 2011). The parameter M_{th} describes the mass below which the thermal density distribution dominates. For a core with surface density $\Sigma = M_{\star,f}\epsilon_{core}^{-1}/\pi R_{core}^2$, M_{th} is defined as

$$M_{th} = 1.23 \times 10^{-3}\left(\frac{T}{20\,K}\right)^3 \left(\frac{30\epsilon_{core} M_\odot}{M_{\star,f}}\right)^{1/2} \Sigma_0^{3/2} M_\odot, \quad (15)$$

where $\Sigma_0 = \Sigma/(1\,g\,cm^{-2})$. We further assume that the accretion rate onto the disk is the same as that onto the star and use this value for our protostellar accretion rate.

3.2.2. Secondary Accretion Phase: Disk Clearing

Late in the formation the core envelope will exhaust its reservoir of mass and no longer feed the accretion disk. We assume that we are left with a thin, Keplerian accretion disk that continues to transfer mass and angular momentum to the central protostar. For simplicity and because observations of disks located around massive stars are very limited, we assume that this results in a decreasing accretion rate as a function of time, which we model as a decaying exponential (Collier Cameron & Campbell 1993; Yi 1994, 1995; Matt et al. 2010):

$$\dot{M}_a = \frac{M_D}{t_a} e^{-t/t_a}, \quad (16)$$

where M_D is the remaining mass in the accretion disk (i.e., the total amount of mass that would accrete from $t = 0 \rightarrow \infty$) and t_a is the decay timescale. Since M_D and t_a are highly unconstrained, we experiment with different values in Section 4. Figure 2 shows the accretion history, including both the core-collapse and disk-clearing accretion phases, for stars with final masses of 0.5–50 $M_\odot$.

3.3. Star–Disk Interaction Model

In Section 2, we showed how the presence of a stellar magnetic field can remove angular momentum from the star as it accretes matter from an accretion disk. This description

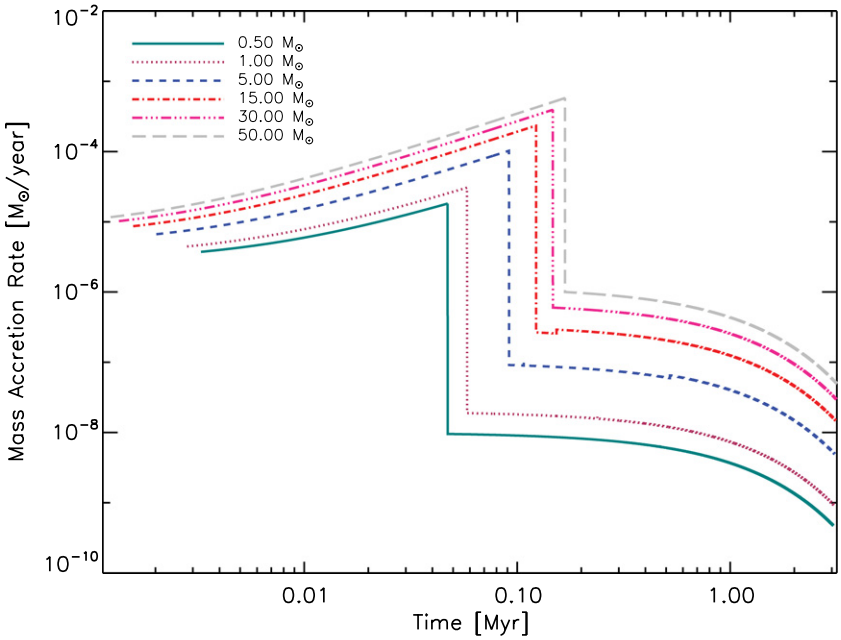

Figure 2. Accretion history of protostars with final masses of 0.5–50 $M_{\odot}$, following Equations (13) and (16), for our fiducial parameters given in Table 1 in Section 4. (A color version of this figure is available in the online journal.)

assumed that the stellar field lines were connected at all radii of the disk larger than $R_{\rm A}$. However, the differential rotation between the star and disk will twist the connected field lines. This twisting will cause the magnetic field to undergo a rapid inflation, leading to an opening of the field lines, effectively decreasing the size of the disk region that is connected to the stellar magnetic field (Lovelace et al. 1995; Uzdensky et al. 2002; Matt & Pudritz 2005). We now include this effect when calculating the net magnetic torque on the star with the use of the model developed by MP05, which is an extension to the disk-locking model first developed by Ghosh & Lamb (1978) for accreting neutron stars and extended by Koenigl (1991) to describe the star–disk coupling for magnetized T Tauri stars.

3.3.1. Magnetic Coupling to the Disk and the Connection State

The effect of the opening of the magnetic field lines depends on the strength of the magnetic coupling to the disk and how strongly the field lines can be twisted until they are severed. The variable $\gamma(r) = B_{\phi}/B_z$ describes the twisting of the magnetic field between the star and disk. This twisting occurs rapidly so a steady-state configuration depends on how well the field couples to the disk (i.e., the balance between the differential rotation and the tendency for the magnetic field to untwist). Uzdensky et al. (2002) describe this coupling by a dimensionless magnetic diffusivity parameter,

$$\beta \equiv \frac{\eta_{\rm t}}{H v_{\rm k}}, \tag{17}$$

where η_t is the effective magnetic diffusivity and is of the order of magnitude of the disk's effective viscosity (Lovelace et al. 1995), H is the scale height of the disk, and v_k is the Keplerian rotation velocity. MP05 assume that β is constant throughout the disk. The field is strongly coupled to the disk for values of $\beta < 1$ and weakly coupled for $\beta > 1$. Uzdensky et al. (2002) find that when γ exceeds a value of order unity (defined by the critical twist parameter γ_c) the magnetic field will be severed because the magnetic pressure force associated with B_{ϕ} will push outward and cause the dipole field loops to open. The magnetic field is connected to the disk only in the location where $|\gamma| \leqslant \gamma_c$. MP05 use the values $\beta = 0.01$ and $\gamma_c = 1$ in their models, and we adopt the same fiducial values in this work. They suggest that $\beta = 0.01$ is the most probable value for a T Tauri accretion disk with the use of an α model prescription; however, it is uncertain that disks surrounding massive stars will have this same value. For example, massive stars emit more ionizing radiation, which will yield a higher ionization fraction on the disk surface, causing β to decrease, but these disks are also more massive than those surrounding low-mass PMS stars and are therefore thicker, causing β to increase. To account for our uncertainty in this parameter, we experiment with different values in the following section.

MP05 show that the magnetic connection between the star and disk changes at a threshold value of the stellar spin rate. Specifically, the stellar magnetic field will only be connected to a small region of the disk within $R_{\rm co}$ if the stellar rotation rate as a fraction of breakup,

$$f = \frac{\Omega_{\star}}{\Omega_{\rm bu}} = \Omega_{\star}\sqrt{\frac{R_{\star}^3}{GM_{\star}}}, \tag{18}$$

falls below

$$f < (1 - \beta\gamma_c)(\gamma_{\rm c}\psi), \tag{19}$$

where

$$\psi \equiv \frac{2B_{\star}^2 R_{\star}^{5/2}}{\dot{M}_{\rm a}\sqrt{GM_{\star}}} \tag{20}$$

is a dimensionless parameter that relates the strength of the magnetic field to the accretion rate. This connection state, which MP05 denote as state 1, will result in no spin-down torques transferred to the star. If f exceeds this value, then the system is in state 2, which is characterized by a magnetic connection on either side of $R_{\rm co}$ resulting in both spin-up and spin-down torques acting on the star.

3.3.2. Magnetic and Accretion Torques

The twisting of the magnetic field by the differential rotation between the star and disk causes torques to be conveyed between the two. The twisting of the magnetic field within R_{co} leads to spin-up torques, whereas the field lines connected to the disk outside of R_{co} act to spin down the star. If the magnetic field is strong enough, then the disk will be disrupted by the stellar magnetosphere where the magnetic stress is able to maintain the accretion rate within the disk. At this location, denoted by R_t, the magnetic stress is large enough to remove the excess angular momentum and funnel the disk material along the magnetic field lines. This material and its angular momentum are transferred to the star. If $R_t > R_{co}$, the magnetic stress hinders the accretion rate.

The location of R_t depends on the connection state of the system. In state 1 the truncation radius is

$$R_t = (\gamma_c \psi)^{2/7} R_\star. \tag{21}$$

In state 2 the truncation radius is given by

$$\left(\frac{R_t}{R_{co}}\right)^{-7/2}\left[1-\left(\frac{R_t}{R_{co}}\right)^{3/2}\right] = \frac{\beta}{\psi f^{7/3}}. \tag{22}$$

We assume that the accreted disk material is quickly integrated into the structure of the star and adds angular momentum to the star at a rate given by Equation (6), where R_A is replaced by R_t. This material acts to spin up the star.

The magnetic connection over a range in radii in the disk can extract angular momentum from the star and transfer it to the disk. If the system is in state 2, then the magnetic field is connected to the disk from R_t to $R_{out} = (1+\beta\gamma_c)^{2/3} R_{co}$, which yields a net magnetic torque on the star:

$$\tau_m = \frac{B_\star^2 R_\star^6}{3\beta R_{co}^3}\left[2(1+\beta\gamma_c)^{-1} - (1+\beta\gamma_c)^{-2} - 2(R_{co}/R_t)^{3/2} + (R_{co}/R_t)^3\right]. \tag{23}$$

If the system is in state 1, then the magnetic field is connected to only a small portion of the disk, which leads to a negligible torque on the star, so we set $\tau_m = 0$ following Matt et al. (2010). Note that Equation (23) reduces to Equation (5) for the limiting case of no field opening ($\gamma_c \to \infty$), marginal coupling ($\beta = 1$), and a disk that is truncated at the Alfvén radius (R_A) and extends to infinity.

4. RESULTS

The initial star-forming core properties are determined by the core mass (M_{core}), core density profile (k_ρ), and core surface density (Σ). These parameters control the accretion rate for the primary accretion phase as described in Section 3.2.1. We initially create a "pre-collapse" object with a mass less than 0.01 $M_\odot$, which grows in mass with the accretion rate given by Equation (13). When the object reaches a mass of 0.01 $M_\odot$, we initialize our protostellar and angular momentum evolution model and assume that the protostar is initially rotating at 1% of its breakup speed. When the protostar is initialized, it is immediately spun up since the accretion rate is large, so our chosen value for the initial rotation speed is unimportant. We solve Equation (11) with the fourth-order Runge–Kutta scheme of Press et al. (2007) and update the angular momentum of the star by computing the net torque on the star arising from the accretion and magnetic torques described in Section 3.3.2. We use this result to update $\Omega_\star$. We cap the stellar rotation rate at 50% of breakup, a limit imposed by gravitational torques (Lin et al. 2011). The fiducial values used for our model parameters are given in Table 1.

Table 1
Table of Fiducial Values Used for Our Model Parameters

Parameter	Fiducial Value
Σ	1 g cm^{-2}
M_D	0.02 $M_{\star,f}$
t_a	10^6 yr
$B_\star$	2 kG
β	0.01
γ_c	1

4.1. Effect of the Star–Disk Magnetic Interaction

Figure 3 shows the radial and rotational evolution for stars ranging in final stellar mass from 0.5 to 50 $M_\odot$. These models were simulated with the fiducial parameters given in Table 1. The disk-clearing accretion phase is assumed to last 3 Myr, although as discussed in Section 1, this assumption is almost certainly not correct for high-mass stars. As we show below, using a shorter disk-clearing timescale for the massive stars would only strengthen our results. We choose to run the disk-clearing phase for three decay timescales because accretion disks around low-mass stars survive for several million years (Herbst et al. 2007), with an accretion rate that likely decreases with time. The swelling in radius by a factor of three, shown in the upper plots of Figure 3, is a result of the star transitioning from a convective to radiative core (Hosokawa & Omukai 2009), which redistributes entropy within the star. For the stars presented in Figure 3 this occurs in the primary accretion phase for the most massive stars ($M_{\star,f} \geqslant 15\ M_\odot$) and during the disk-clearing accretion phase for the 0.5, 1, and 5 $M_\odot$ stars. If the jump in radius occurs during the main accretion phase, it causes the star to immediately slow down, but the star is almost instantly spun back up because of the high accretion rate. In the case of the 5 $M_\odot$ star, this jump in radius also significantly decreases the spin rate of the star, but since it occurs when the accretion rate is much lower, the star only gradually spins up as it contracts and accretes material. In contrast, for the 0.5 and 1 $M_\odot$ stars magnetic torques are able to continue to spin down the star after the jump in radius occurs. We note that Matt et al. (2010) produced Sun-like stars with faster rotation rates (~20%–40% of breakup) performing a similar analysis. We report a lower rotation rate for our 1 $M_\odot$ protostar because it has a different radial history than the stars produced by Matt et al. (2010). Our 1 $M_\odot$ protostar contracts more slowly than the 1 $M_\odot$ protostar model used by Matt et al. (2010). After 3 Myr, our model gives a radius of 3.8 $R_\odot$ as compared to Matt et al.'s (2010) ~3 $R_\odot$. At times <1 Myr, the model radii can differ by factors of ~2. The larger radii in our model produce more spin-down. The differences in predicted radii likely arise because our model accounts for the extra entropy provided both by deuterium burning and by ongoing accretion, while Matt et al.'s (2010) does not. We do warn, however, that there are significant uncertainties in how much of the accretion entropy is actually absorbed by the star, and differing assumptions on this point can produce significant differences in radial evolution (Hosokawa et al. 2011).

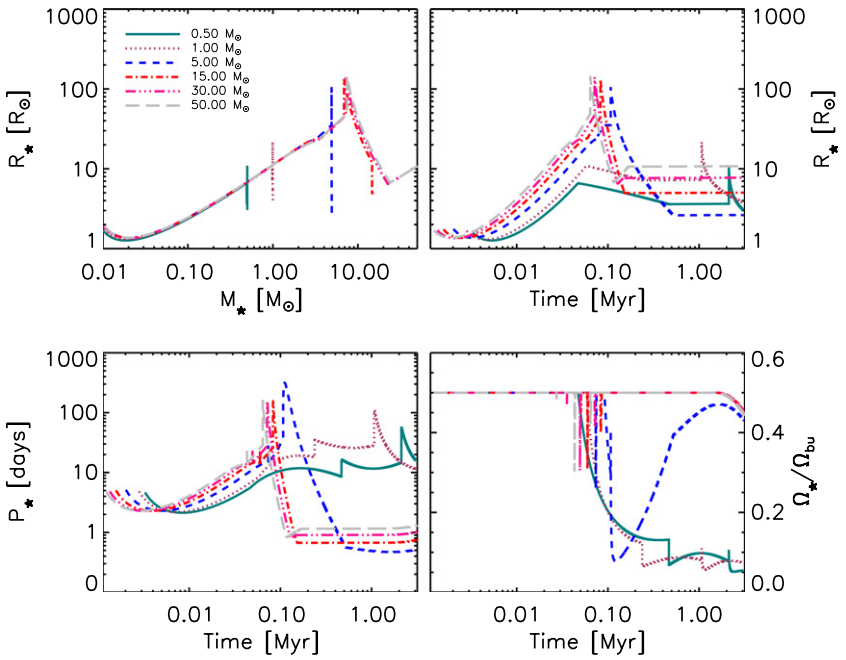

Figure 3. Top left panel shows the stellar radius as a function of stellar mass for stars with masses 0.5–50 $M_{\odot}$. The other panels show the stellar radius (top right), stellar period (bottom left), and stellar spin rate as a fraction of breakup (bottom right) as a function of time for stars with masses 0.5–50 $M_{\odot}$. Figure 2 shows the accretion histories.

(A color version of this figure is available in the online journal.)

We find that the torques that arise from the star–disk magnetic interaction are unable to spin down both low-mass and massive protostars during the main accretion phase but are important during the disk-clearing phase, especially for low-mass stars. Low-mass stars begin to spin down the instant the disk-clearing accretion phase begins, whereas it takes approximately 2 Myr to begin to spin down massive stars for our chosen fiducial values. This suggests that massive stars are difficult to spin down due to their larger inertia and because their magnetic fields are weaker relative to their stellar binding energy as compared to low-mass stars.

Figure 4 shows snapshots of the stellar radius, disk truncation radius, stellar period, and stellar rotation rate as a fraction of breakup as a function of stellar mass taken at different times during the disk-clearing phase. First consider the upper left panel, showing radius versus mass at different times. The R–M relation toward which the models converge at high mass is the ZAMS; by 3 Myr all stars above $\sim 2\,M_{\odot}$ have reached it. At smaller masses, the maximum radius occurs at a mass that corresponds to stars that have just made the convective-radiative core transition at a given time. This value shifts to progressively smaller masses at later times.

An interesting feature of Figure 4 is that the stellar rotation rates as a fraction of breakup show a bimodal distribution: stars with $M_{\star,\mathrm{f}} \lesssim 1\ M_{\odot}$ rotate at $\sim$10% of their breakup speed, whereas stars with $M_{\star,\mathrm{f}} \gtrsim 6\,M_{\odot}$ are rapid rotators. In between these plateaus (i.e., the "transition region") the rotation rates as a fraction of breakup increase with stellar mass. Furthermore, as time increases we find that the ratio of rotation speed to breakup speed decreases on both plateaus, but that this decrease is more noticeable for the fast rotator plateau. This is because the stars located on the fast rotator plateau have already reached the ZAMS and are no longer contracting, whereas those located on the slow rotator plateau are easy to spin down because of their low inertia, even though they are still contracting toward the ZAMS. In contrast, we find that the rotation rates as a fraction of breakup of the stars in the transition region increase with time. This suggests that the magnetic torques conveyed by the star–disk interaction are unable to counteract the increase in the stellar spin rate due to contraction for stars in the transition region. However, once these stars have reached the ZAMS magnetic torques do become important. The points located in the bottom right panel of Figure 4 represent the minimum mass of stars rotating at $\gtrsim$20% of their breakup speed. We use this as an indicator of the transition between slow and fast rotators, which we discuss further in Section 4.3.

4.2. Sensitivity to Model Parameters

In the previous subsection, we found that massive stars are much more difficult to spin down than low-mass stars. This causes low-mass stars to become slow rotators and massive stars to be rapid rotators, yielding a bimodal distribution in stellar rotation speeds as a fraction of the breakup speed. To explore if this qualitative result is sensitive to our chosen model parameters, we vary certain parameters while holding the other parameters fixed. In the figures that follow we see that by varying certain parameters we do not lose this feature, but only alter it.

4.2.1. Varying Σ

Figure 5 shows the final stellar radius, disk truncation radius, stellar period, and rotation rate as a fraction of breakup as a function of final stellar mass for different values of the initial core surface density, Σ. The accretion rate during the main accretion phase increases for higher Σ, so varying this value affects the accretion history only during this phase. We find that this parameter has little to no effect on the final spin rate of the stars because the magnetic torques are unimportant during this accretion phase. The very minor differences that do appear arise because the value of Σ affects the time at which a star of a given final mass reaches the swelling phase: the swelling phase of the star occurs earlier in time at lower Σ. For each value of Σ used in

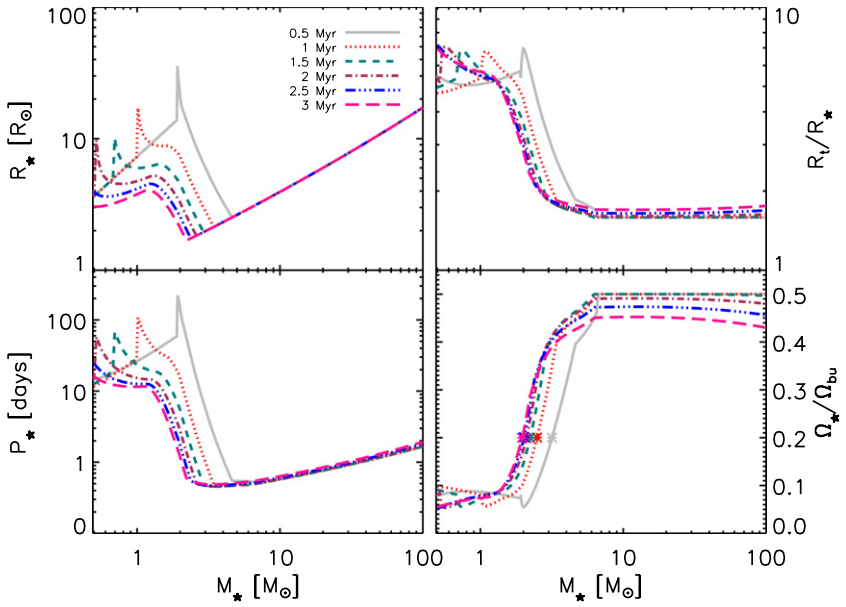

Figure 4. Snapshots of the stellar radius (upper left), disk truncation radius (upper right), stellar period (lower left), and rotation rate as a fraction of breakup (lower right) as a function of stellar mass taken at different times during the disk-clearing phase for our fiducial case. The times in the legend represent the time that has elapsed since the disk-clearing phase began. The points located in the bottom right panel represent the minimum mass of stars rotating at $\gtrsim$20% of its breakup speed. We use this as an indicator of the transition between slow and fast rotators.

(A color version of this figure is available in the online journal.)

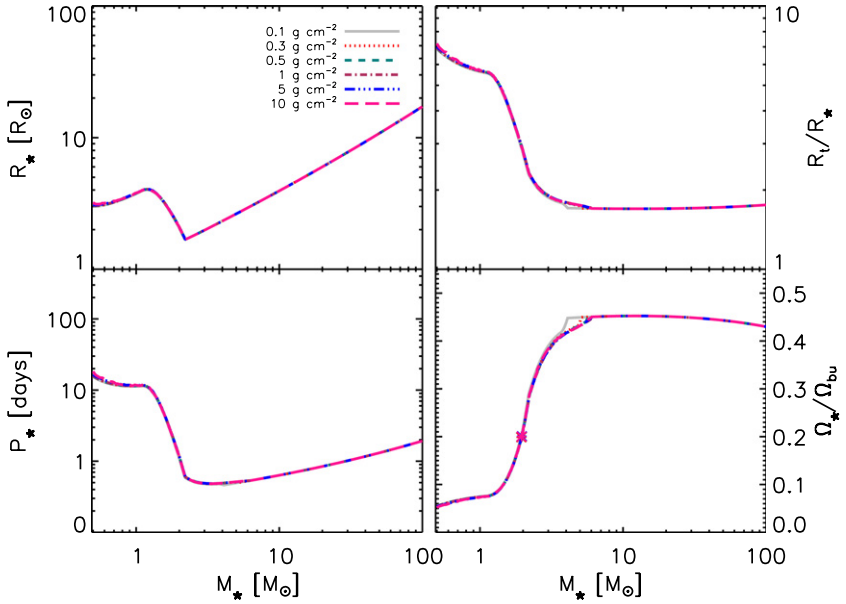

Figure 5. Same as Figure 4, but all quantities are shown at a time of 3 Myr, and we vary Σ as indicated in the legend.

(A color version of this figure is available in the online journal.)

our models there is a slight kink in between $M_{\star,\mathrm{f}} \approx 3$ and $6\,\mathrm{M}_{\odot}$ and the location of this kink decreases in mass for smaller values of Σ. Stars to the right of this kink experience the jump in radius, discussed in Section 4.1, before the end of the main accretion phase, whereas those to the left experience the swelling during the disk-clearing accretion phase. However, the net effect on the stellar rotation rate is obviously minor.

4.2.2. Varying M_D

Figure 6 shows the final stellar radius, disk truncation radius, stellar period, and rotation rate as a fraction of breakup as a function of final stellar mass for different values of the initial disk mass, M_{D}, used for the disk-clearing accretion phase. Increasing M_{D} increases the accretion rate during the disk-clearing phase, thus increasing the accretion torque. A larger accretion rate also causes the disk to be truncated closer to the star, effectively reducing the net spin-down magnetic torque. This is because the stellar magnetic field lines will connect to a greater portion of the disk within R_{co}, yielding greater spin-up magnetic torques on the star, while the magnetic spin-down torques remain unchanged. We find that altering M_{D} changes the location and shape of the transition between the slow and fast rotation plateaus, but the qualitative result that rotation rates are bimodal, with slow rotation at low mass and rapid rotation

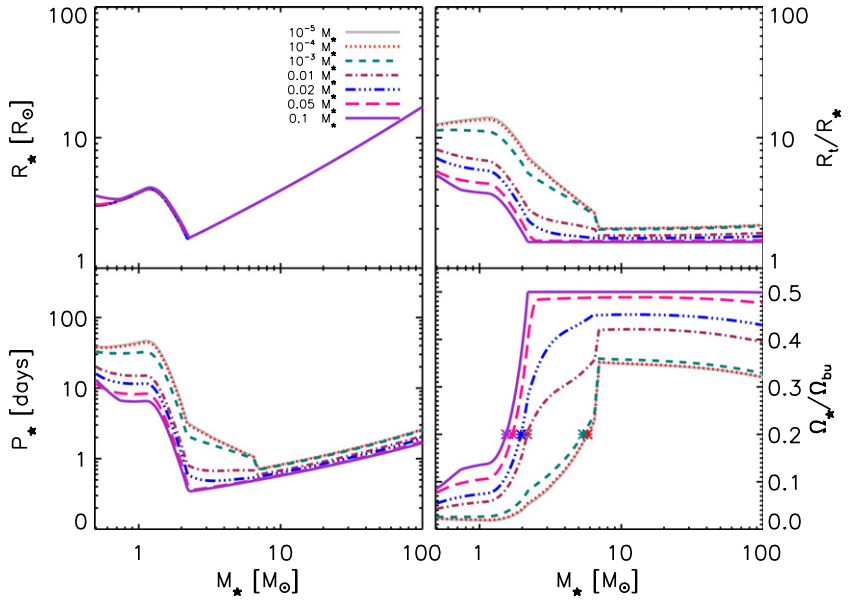

Figure 6. Same as Figure 4, but all quantities are shown at a time of 3 Myr, and we vary M_D as indicated in the legend.
(A color version of this figure is available in the online journal.)

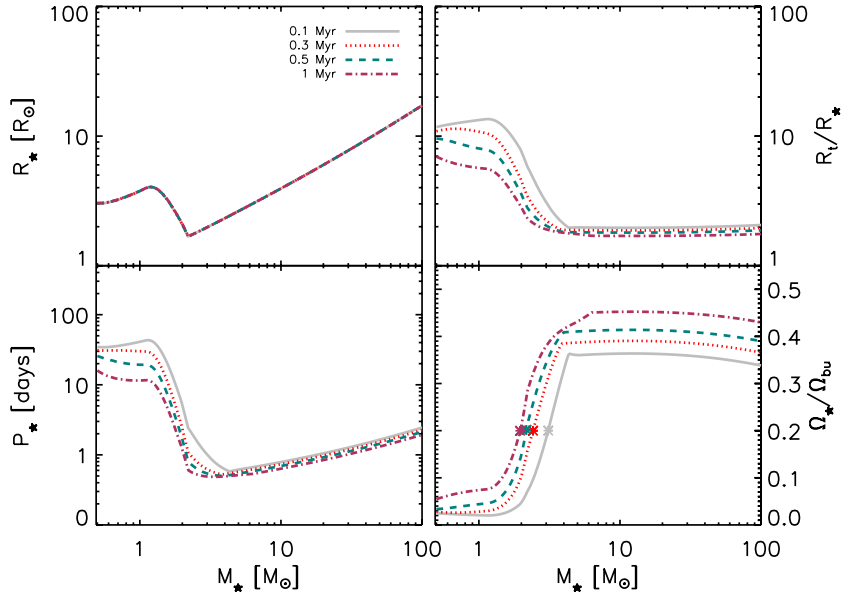

Figure 7. Same as Figure 4, but all quantities are shown at a time of 3 Myr, and we vary t_a as indicated in the legend.
(A color version of this figure is available in the online journal.)

at high mass, remains unchanged. Also note that the models converge in the limit $M_D \rightarrow 0$.

4.2.3. Varying t_a

Figure 7 shows the final stellar radius, disk truncation radius, stellar period, and rotation rate as a fraction of breakup as a function of final stellar mass for different values of the disk decay timescale, t_a, used for Equation (16). Smaller values of t_a, as compared to our fiducial value of 1 Myr, correspond to a higher initial accretion rate that declines more rapidly for the disk-clearing accretion phase. This yields lower final spin rates at the end of 3 Myr. However, the overall shape of the distribution of final spin rates as a function of stellar mass does not change.

4.2.4. Varying $B_\star$

Figure 8 shows the final stellar radius, disk truncation radius, stellar period, and rotation rate as a fraction of breakup as a function of final stellar mass for different values of the stellar magnetic field strength. Clearly, a larger magnetic field strength provides a greater spin-down torque on the star, yielding smaller final spin rates as a function of mass. As can be seen in this figure, stars above $M_{\star,f} \gtrsim 2\ M_\odot$ require surface fields greater than 1 kG to experience any significant spin-down torques and do not become slow rotators, $\Omega_\star/\Omega_{bu} \lesssim 0.1$, unless the field reaches $\sim$10 kG. Magnetic fields this large have only been detected in the chemically peculiar (e.g., helium strong) Ap/Bp stars (Borra & Landstreet 1979; Oksala et al. 2010). Generally, as the field strength increases, the final spin rates decrease, but

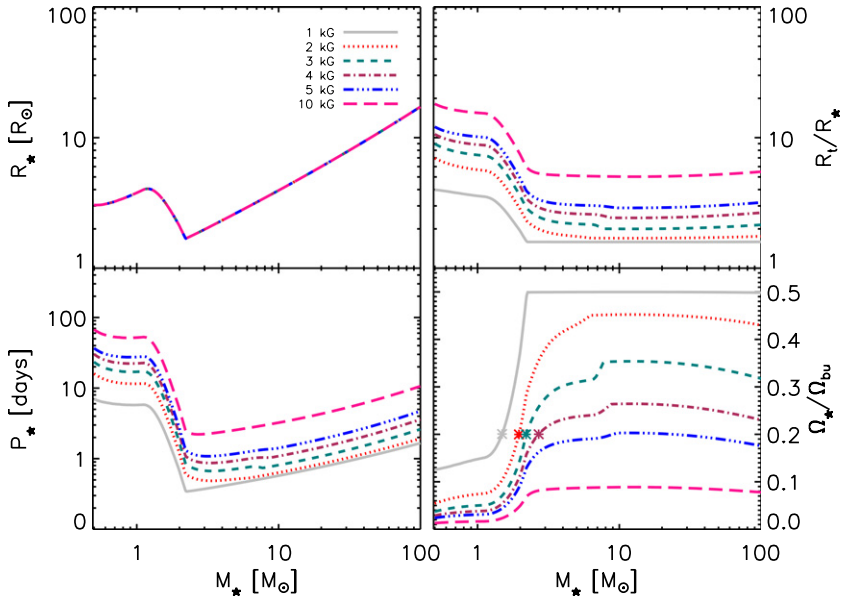

Figure 8. Same as Figure 4, but all quantities are shown at a time of 3 Myr, and we vary $B_\star$ as indicated in the legend.
(A color version of this figure is available in the online journal.)

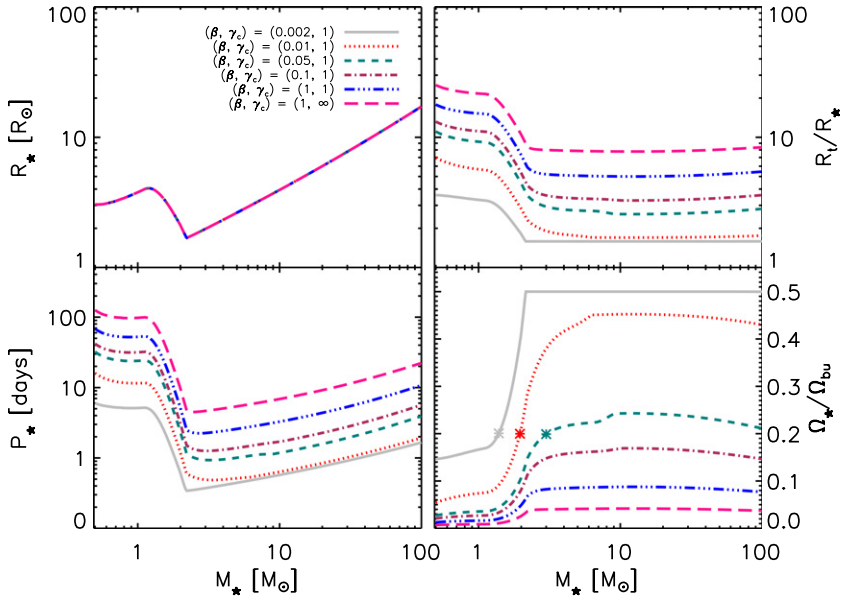

Figure 9. Same as Figure 4, but all quantities are shown at a time of 3 Myr, and we vary β and γ_c as indicated in the legend.
(A color version of this figure is available in the online journal.)

the qualitative division between slow and fast rotators remains. We also find that this same trend in rotation rates as a fraction of breakup occurs as the field lines become weakly coupled to the accretion disk, while holding the magnetic field strength fixed, as discussed next.

4.2.5. Varying β and γ_c

Figure 9 shows the final stellar radius, disk truncation radius, stellar period, and rotation rate as a fraction of breakup as a function of final stellar mass for different values of β and γ_c. These parameters describe the coupling and connection of the stellar magnetic field lines to the accretion disk (i.e., the location where the field lines open and disconnect from the disk). A larger β for a given γ_c increases the extent of the connected disk region. This is because the coupling of the stellar field lines to the disk acts to resist the twisting of these lines due to the differential rotation between the star and disk. Thus, weaker field coupling will lead to a greater spin-down torque acting on the star, leading to lower rotation rates as depicted in Figure 9. Likewise, a greater γ_c for a given β will allow the field lines to experience a greater twist before opening, also increasing the size of the connected disk region. For the case where $\gamma_c \rightarrow \infty$ (i.e., field lines are allowed to twist to large values without opening), the field lines will connect to the whole disk outside R_t. This will lead to a greater spin-down torque. The case where $\beta = 1$ and $\gamma_c = \infty$ reduces to the case described in Section 2. Figure 9 shows that as β increases for $\gamma_c = 1$, all stars have lower rotation rates. However, the two plateaus still remain.

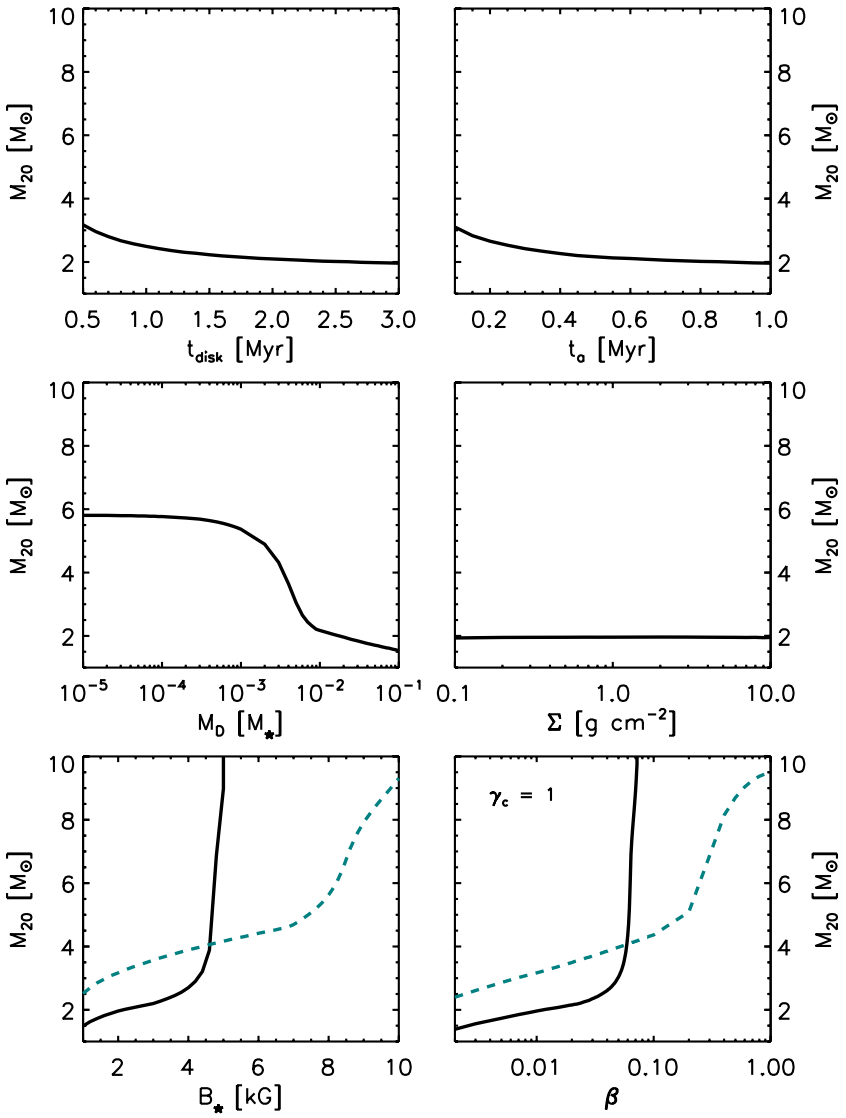

Figure 10. Sensitivity of the model parameters. The *y*-axes show the minimum stellar mass where $f \geqslant 0.2$, denoted as M_{20}, for different parameters as indicated on the *x*-axes. Except for the top left plot, the black solid lines indicate that these values were taken for a disk lifetime of 3 Myr. In the bottom panels, the teal dashed lines show the value of M_{20} 0.5 Myr after the beginning of the disk-clearing phase for comparison.

(A color version of this figure is available in the online journal.)

4.3. The Characteristic Mass for the Slow-to-Fast Rotator Transition

In this work, we have found a robust division between slow and fast rotators. Specifically, we find that low-mass stars (e.g., stars with $M_\star \lesssim 1\,M_\odot$) are slow rotators, easily spun down via magnetic torques that arise from the star–disk interaction, and rotate at ∼10% of their breakup speed, whereas massive stars (e.g., $M_\star \gtrsim 6\,M_\odot$) are preferentially fast rotators. This is because massive stars are difficult to spin down due to their larger inertia and because their magnetic fields are weaker relative to their stellar binding energy as compared to low-mass stars. Furthermore, this division is also dependent on the *R–M* relationship. The stars located on the fast rotator plateau have reached the ZAMS by the end of the main accretion phase or early on during the disk-clearing phase, whereas the stars located on the slow rotator plateau are shrinking toward the ZAMS for the entirety of the disk-clearing phase. Likewise, the stars located in the transition region are contracting toward the ZAMS for a significant portion of the disk-clearing phase but are contracting much faster than the low-mass slow rotators, leading to the sudden rise in rotation rates as a fraction of breakup.

To further illustrate the division between slow and fast rotators for each of our model parameters, in Figure 10 we plot the minimum stellar mass at which the star ends accretion rotating at 20% of its breakup speed, which we call M_{20}. Each panel shows how M_{20} depends on the individual parameters in our model (while setting the other parameters to their fiducial values). The top panels show that M_{20} decreases by only a small amount as the disk lifetime (i.e., the amount of time the disk survives and supplies mass to the star during the disk-clearing phase) or disk decay timescale increases. We also see that this characteristic mass, as a function of the initial core surface density, is relatively constant as indicated by the nearly horizontal line in the middle right panel of Figure 10. In contrast, M_{20} spans a larger mass range as we vary the initial disk mass used for the secondary accretion phase as shown in the middle left panel. This is because the accretion rate, and therefore the accretion torque, is proportional to the disk mass used in our model. We find

that as $M_D \rightarrow 0$ the values of M_{20} become constant, but we note that M_{20} decreases most as the disk mass increases from $\sim 10^{-3}$ to $10^{-2}\ M_\star$. The division between slow and fast rotators slowly decreases in stellar mass for initial disk masses above $\sim 10^{-2}\ M_\star$. Even though varying this parameter leads to larger variations in M_{20} as compared to the top panels, it does not change the qualitative division between slow and fast rotators.

The bottom panels of Figure 10 show how the slow–fast rotator division is affected by the stellar magnetic field strength and the coupling of the stellar magnetic field lines to the disk, which are the parameters that are responsible for the removal of angular momentum from the star. The black solid lines in these panels show that the division between the slow and fast rotators (i.e., M_{20}) diverges for large magnetic field strengths ($B_\star \gtrsim 4.5$ kG) or weak field coupling ($\beta \gtrsim 0.05$) for a disk-clearing accretion phase that lasts for 3 Myr. This is because no stars will be rotating at or above 20% of their breakup speed at the end of 3 Myr for such high values of $B_\star$ or β. For comparison, and also because we expect disks to have shorter lifetimes around massive stars, we also include the values of M_{20} at 0.5 Myr after the disk-clearing phase began (teal dotted lines). We find that M_{20} is larger at shorter times because these stars are still contracting toward the ZAMS. At 0.5 Myr stars with masses greater than $\sim 5\ M_\odot$ have reached the ZAMS, as indicated by the kink and faster increase of M_{20} in these plots for the 0.5 Myr case.

5. DISCUSSION

We have shown that massive stars are fast rotators at birth and that their initial rotation rates are unlikely to be regulated by the star–disk magnetic interaction. We have found that magnetic torques can only effectively spin down massive stars that have low accretion rates, long disk lifetimes, weak magnetic coupling with the disk, and/or surface magnetic fields that are significantly larger than what current observational estimates suggest. We thus conclude that their initial rotation rates are likely regulated by gravitational torques. Since massive stars arrive on the main sequence as fast rotators, their variation in rotation rates as a fraction of their breakup rate is likely a result of evolutionary spin-down, due to stellar expansion and/or angular momentum loss via stellar winds while on the main sequence.

5.1. Observational Implications

A topic of current debate is whether the distribution of the projected rotational velocities of massive stars depends on birth environment or if this property is only affected by evolutionary spin-down (Strom et al. 2005; Dufton et al. 2006; Huang & Gies 2006, 2008; Wolff et al. 2007, 2008; Huang et al. 2010). Strom et al. (2005) observed the rotational velocities of B stars located in high stellar density clusters and compared them to field stars of similar age (∼12–15 Myr). They found that, on average, the cluster stars had larger rotational velocities than the field stars in their sample and that only the most evolved cluster stars had similar rotational velocities as their field star counterparts. Likewise, Wolff et al. (2007, 2008) observed that massive stars (e.g., $M_\star \gtrsim 6\ M_\odot$) found in clusters characterized by a high stellar density are faster rotators than their similar mass counterparts located in lower density clusters. These studies concluded that the initial spin rates of these stars depend on the initial star-forming environment since these stellar ensembles, which have survived as bound clusters, likely form in molecular clouds characterized by high surface densities. Furthermore, Wolff et al. (2007) compared the distribution of the rotational velocities of B stars in both young and older high-density and low-density environments and did not detect a significant evolutionary change.

In agreement, Huang et al. (2010) compared the rotation rates of cluster and field B stars and found that, on average, cluster stars tend to rotate faster than field stars. However, by grouping the stars by surface gravity, an age proxy, they found that there is little difference between the average rotational velocities for the field and cluster stars as a function of age, and that they exhibit a similar spin-down with advanced evolution. They also found that field stars are in general more evolved than cluster stars. These results suggest that the observed trend in the rotational velocities of B stars is due to evolutionary spin-down rather than to the initial conditions of the environment in which they formed. They argue that the discrepancy between the average rotation rate of the field stars and cluster stars in their sample is that the field stars have undergone evolutionary spin-down since the field star sample contained more evolved stars.

For a fixed surface magnetic field strength, we find here that the initial rotation rates of massive stars, due to disk locking, have no dependence on the environmental density. As described in Section 3.2.1, the accretion rate during the main accretion phase does depend on the star-forming environment, with larger surface density yielding a greater time-averaged accretion rate. Wolff et al. (2007) proposed that the higher rotation rates they report for stars in dense clusters are the result of disk locking plus a systematically higher accretion rate in dense clusters. However, we find that magnetic torques are insignificant during the main accretion phase regardless of environment density because of the high accretion rates. These torques only become important during the disk-clearing phase, and there is no obvious reason that the properties or behavior of the disk during this phase should depend on the environment. However, this does not rule out other factors that may depend on the environment. In this work, we assumed that all stars had the same surface magnetic field strength. If the strength of the magnetic fields present during the star formation process depends on environment, either because the star-forming cloud has a different magnetic mass-to-flux ratio and/or because the ambipolar diffusion process depends on density, then this could provide a viable explanation for the difference in rotational velocities of young stars in environments of varying density. Another possibility for the difference in rotational velocities of stars born in different environments may be related to the lifetimes of disks in such environments. We have found that the rotation rates of these stars depend crucially on the lifetime of the accretion disk. Thus, if disks have shorter lifetimes in higher stellar density environments, possibly due to tidal dissipation from interactions with neighbors or rapid photoevaporation due to radiation from nearby massive stars, then the initial rotation rates of these stars will only increase as they contract toward the ZAMS (Wolff et al. 2007).

5.2. Future Work and Caveats

In this work, we have omitted two potentially important effects: that magnetic fields might be stronger early in stars' lives and that stars can be spun down by winds on the main sequence. As mentioned in Section 1, magnetic fields in massive stars are likely to be the decaying remnants of magnetic flux swept up during the star formation process. Therefore, it is plausible that accreting massive stars have stronger magnetic fields than those

we observe as main-sequence O and B stars. If this is the case, then massive stars will likely be spun down via magnetic torques. If the decay process is the same for all stars, then we expect that the strongest magnetic fields should be observed in the slowest rotators. However, we also discovered that the spin rates of these stars depend heavily on how well the stellar magnetic field lines couple to the accretion disk. As described in Section 3.3.1, the true value of β is highly uncertain because it depends on the microphysics of the accretion disk. Since observations of disks around massive stars are rare, we are unable to provide a confident estimate for β. However, by exploring a range of values for β, we have determined that if the field lines are weakly coupled to the disk, then magnetic torques can sufficiently spin down massive stars. Also, measuring the rotation rates of young, massive stars can provide a better estimate for β. If the slowest rotators prove to have weak magnetic fields, then it may be likely that the field lines were weakly coupled to the disk, resulting in a larger β, thus producing these slower rotators.

Stars on the main sequence also shed mass and angular momentum via stellar winds, which we have neglected in this work. In the presence of a stellar magnetic field, these winds will couple with the field lines, causing the star to lose a significant amount of angular momentum as it evolves (Weber & Davis 1967). Since the mass-loss rates of stars increase with stellar mass (Nieuwenhuijzen & de Jager 1990), more massive stars will lose angular momentum at a greater rate. If the spin rates of massive stars are regulated by gravitational torques rather than magnetic torques produced by the star–disk magnetic interaction, then we expect that all massive stars should be rotating at ∼50% of their breakup speed once they are deposited on the ZAMS, assuming that their disks survive long enough. Spin-down will occur as they evolve and shed angular momentum via stellar winds. This is consistent with the results of Huang et al. (2010), who found that young stars with masses greater than $\sim 2\,M_{\odot}$ are preferentially fast rotators and that the average rotation speed as a fraction of the breakup speed, for each mass bin, decreases for increasing stellar mass.

A.L.R. acknowledges support from the NSF GRFP. M.R.K. is supported by the Alfred P. Sloan Foundation, the NSF through grant CAREER-0955300, and NASA through grant NNX09AK31G and a Chandra Telescope grant. E.R.R. acknowledges support from the David and Lucille Packard Foundation and NSF grant: AST-0847563. A.L.R. thanks Nathan Goldbaum, James Guillochon, Nic Ross, and Rachel Strickler for useful discussions. We thank the editor and the referee for taking the time to carefully read our manuscript and provide useful comments.

REFERENCES

Alecian, E., Wade, G. A., Catala, C., et al. 2008, A&A, 481, L99
Armitage, P. J., & Clarke, C. J. 1996, MNRAS, 280, 458
Beuther, H., Schilke, P., Menten, K. M., et al. 2002, ApJ, 566, 945
Bjorkman, J. E., & Cassinelli, J. P. 1993, ApJ, 409, 429
Bodenheimer, P. 1995, ARA&A, 33, 199
Borra, E. F., & Landstreet, J. D. 1979, ApJ, 228, 809
Bouvier, J. 2007, in IAU Symp. 243, Star-Disk Interaction in Young Stars, ed. J. Bouvier & I. Appenzeller (Cambridge: Cambridge Univ. Press), 231
Caselli, P., & Myers, P. C. 1995, ApJ, 446, 665
Cesaroni, R., Galli, D., Lodato, G., Walmsley, M., & Zhang, Q. 2006, Nature, 444, 703
Cesaroni, R., Galli, D., Lodato, G., Walmsley, C. M., & Zhang, Q. 2007, in Protostars and Planets V, ed. B. Reipurth, D. Jewitt, & K. Keil (Tucson, AZ: Univ. Arizona Press), 197
Chini, R., Hoffmeister, V. H., Nielbock, M., et al. 2006, ApJ, 645, L61
Chini, R., Hoffmeister, V. H., & Nürnberger, D. 2011, Bull. Soc. R. Sci. Liege, 80, 217
Collier Cameron, A., & Campbell, C. G. 1993, A&A, 274, 309
Crutcher, R. M. 1999, ApJ, 520, 706
Cunningham, A. J., Klein, R. I., Krumholz, M. R., & McKee, C. F. 2011, ApJ, 740, 107
Davies, B., Hoare, M. G., Lumsden, S. L., et al. 2011, MNRAS, 416, 972
Donati, J.-F., Howarth, I. D., Bouret, J.-C., et al. 2006, MNRAS, 365, L6
Dufton, P. L., Smartt, S. J., Lee, J. K., et al. 2006, A&A, 457, 265
Ghosh, P., & Lamb, F. K. 1978, ApJ, 223, L83
Goodman, A. A., Benson, P. J., Fuller, G. A., & Myers, P. C. 1993, ApJ, 406, 528
Grunhut, J. H., Wade, G. A., Marcolino, W. L. F., et al. 2009, MNRAS, 400, L94
Hartmann, L., D'Alessio, P., Calvet, N., & Muzerolle, J. 2006, ApJ, 648, 484
Hartmann, L., & Stauffer, J. R. 1989, AJ, 97, 873
Herbst, W., Eislöffel, J., Mundt, R., & Scholz, A. 2007, in Protostars and Planets V, ed. B. Reipurth, D. Jewitt, & K. Keil (Tucson, AZ: Univ. Arizona Press), 297
Hosokawa, T., Offner, S. S. R., & Krumholz, M. R. 2011, ApJ, 738, 140
Hosokawa, T., & Omukai, K. 2009, ApJ, 691, 823
Huang, W., & Gies, D. R. 2006, ApJ, 648, 580
Huang, W., & Gies, D. R. 2008, ApJ, 683, 1045
Huang, W., Gies, D. R., & McSwain, M. V. 2010, ApJ, 722, 605
Hubrig, S., Schöller, M., Schnerr, R. S., et al. 2008, A&A, 490, 793
Johns-Krull, C. M. 2007, ApJ, 664, 975
Koenigl, A. 1991, ApJ, 370, L39
Krumholz, M. R., Klein, R. I., & McKee, C. F. 2007, ApJ, 656, 959
Krumholz, M. R., Klein, R. I., McKee, C. F., Offner, S. S. R., & Cunningham, A. J. 2009, Science, 323, 754
Larson, R. B. 2010, Rep. Prog. Phys., 73, 014901
Lin, M.-K., Krumholz, M. R., & Kratter, K. M. 2011, MNRAS, 416, 580
Lovelace, R. V. E., Romanova, M. M., & Bisnovatyi-Kogan, G. S. 1995, MNRAS, 275, 244
Maeder, A., & Meynet, G. 2010, New Astron. Rev., 54, 32
Martins, F., Donati, J.-F., Marcolino, W. L. F., et al. 2010, MNRAS, 407, 1423
Matt, S. P., Pinzón, G., de la Reza, R., & Greene, T. P. 2010, ApJ, 714, 989
Matt, S., & Pudritz, R. E. 2005, MNRAS, 356, 167
Matzner, C. D., & McKee, C. F. 2000, ApJ, 545, 364
McKee, C. F., & Tan, J. C. 2003, ApJ, 585, 850
Moss, D. 2001, in ASP Conf. Ser. 248, Magnetic Fields across the Hertzsprung-Russell Diagram, ed. G. Mathys, S. K. Solanki, & D. T. Wickramasinghe (San Francisco, CA: ASP), 305
Myers, P. C., & Fuller, G. A. 1992, ApJ, 396, 631
Nakano, T., Hasegawa, T., Morino, J.-I., & Yamashita, T. 2000, ApJ, 534, 976
Nieuwenhuijzen, H., & de Jager, C. 1990, A&A, 231, 134
Offner, S. S. R., Klein, R. I., McKee, C. F., & Krumholz, M. R. 2009, ApJ, 703, 131
Oksala, M. E., Wade, G. A., Marcolino, W. L. F., et al. 2010, MNRAS, 405, L51
Parravano, A., Hollenbach, D. J., & McKee, C. F. 2003, ApJ, 584, 797
Press, W. H., Teukolsky, S. A., Vetterling, W. T., & Flannery, B. P. 2007, Numerical Recipes: The Art of Scientific Computing (Cambridge: Cambridge Univ. Press)
Shu, F. H. 1977, ApJ, 214, 488
Strom, S. E., Wolff, S. C., & Dror, D. H. A. 2005, AJ, 129, 809
Uzdensky, D. A., Königl, A., & Litwin, C. 2002, ApJ, 565, 1191
van der Tak, F. F. S., van Dishoeck, E. F., Evans, N. J., II., & Blake, G. A. 2000, ApJ, 537, 283
Vlemmings, W. H. T., Surcis, G., Torstensson, K. J. E., & van Langevelde, H. J. 2010, MNRAS, 404, 134
Wade, G. A., Fullerton, A. W., Donati, J.-F., et al. 2006, A&A, 451, 195
Walder, R., Folini, D., & Meynet, G. 2011, Space Sci. Rev.
Weber, E. J., & Davis, L., Jr. 1967, ApJ, 148, 217
Wolff, S. C., Strom, S. E., Cunha, K., et al. 2008, AJ, 136, 1049
Wolff, S. C., Strom, S. E., Dror, D., Lanz, L., & Venn, K. 2006, AJ, 132, 749
Wolff, S. C., Strom, S. E., Dror, D., & Venn, K. 2007, AJ, 133, 1092
Yi, I. 1994, ApJ, 428, 760
Yi, I. 1995, ApJ, 442, 768
Zapata, L. A., Palau, A., Ho, P. T. P., et al. 2008, A&A, 479, L25